A Study of Phonon Modes of Magnetic Two-dimensional Materials using Optical Spectroscopy

J. H. Kang[1*,+], Y. Cho[1,+], L. Liang[2,+], X. Kong[2], S. Ghosh[3], F. Kargar[3], C. Hu[4], A. A. Balandin[3], D. Geohegan[2], A. A. Puretzky[2], N. Ni[4], and C. W. Wong[1,*]

[1]*Fang Lu Mesoscopic Optics and Quantum Electronics Laboratory, University of California, Los Angeles, CA 90095, USA*
[2]*Center for Nanophase Materials Sciences, Oak Ridge National Laboratory, Oak Ridge, TN 37831, USA*
[3]*Phonon Optimized Engineered Materials (POEM) Center, Department of Electrical and Computer Engineering, University of California, Riverside, CA 92521, USA*
[4]*Department of Physics and Astronomy and California Nano Systems Institute, University of California, Los Angeles, CA 90095, USA*
** zse0147@ucla.edu, cheewei.wong@ucla.edu*
[+] *J. H. Kang, Y. Cho, and L. Liang contributed equally to this work.*

Abstract: Raman spectroscopy measuring phonon vibration modes of $MnBi_{2n}Te_{3n+1}$ (n=1,2) showed abnormal changes in linewidths of $MnBi_2Te_4$. Out-of-plane force constant was also estimated via Davydov splitting of A_{1g} mode (136 cm^{-1}) of $MnBi_4Te_7$.
OCIS codes: (290.5860) Scattering, Raman; (160.6000) Semiconductor materials; (300.6250) Spectroscopy, condensed matter

1. Introduction

Magnetic topological insulators, which combine topological and magnetic properties, have been of particular interest due to their potential exotic physical states, such as quantum anomalous Hall effect and axion insulator [1]. Accordingly, many researchers have put great effort into combining topological and magnetic properties but have met difficulty in synthesizing materials uniformly. However, the recent breakthrough discovery of $MnBi_2Te_4$, the first-ever intrinsic antiferromagnetic topological insulator created by intercalating bilayer Mn-Te into Bi_2Te_3 crystal structure, has opened the door for active research in this field [2]. The purpose of this study is to explore the phonon modes of $MnBi_{2n}Te_{3n+1}$ (n=1,2) under various conditions using optical spectroscopy. We present our work conducting optical Raman spectroscopy on bulk $MnBi_{2n}Te_{3n+1}$ (n=1,2) at different temperatures and polarization configurations, which were compared with density function theory (DFT) calculations.

2. Material and Method

The bulk $MnBi_{2n}Te_{3n+1}$ (n=1,2) single crystals are prepared by a solution method with Bi_2Te_3 flux [3, 4]. Figure 1 (a) shows a side view of the crystal structure of $MnBi_2Te_4$ (left) and $MnBi_4Te_7$ (middle) as well as the top view of $MnBi_2Te_4$ (top right) which has three-fold symmetry. To achieve clean and flat surfaces for the optical measurements, we mechanically exfoliate the bulk single crystals on Si substrates (Figure 1 (a), bottom right). The average thickness of the flakes is thicker than 100 nm. We use a narrow bandwidth laser with 532.2 nm wavelength, with a Mitutoyo 80× objective lens at a power below 1.5 mW. The Raman spectrum is acquired with a Horiba 1000M spectrometer with 1200 grooves/mm grating and the spectrometer is calibrated with a Mercury lamp and Si peak at 520 cm^{-1} at room temperature prior to the measurements. The samples are kept in a helium cryostat, Janis ST-500. We use λ/2 and λ/4 waveplates to generate linear and circular polarizations of the incident laser, respectively. Two Ondax notch filters suppress the laser Rayleigh scattering and reveal low-frequency Raman peaks down to 30 cm^{-1}.

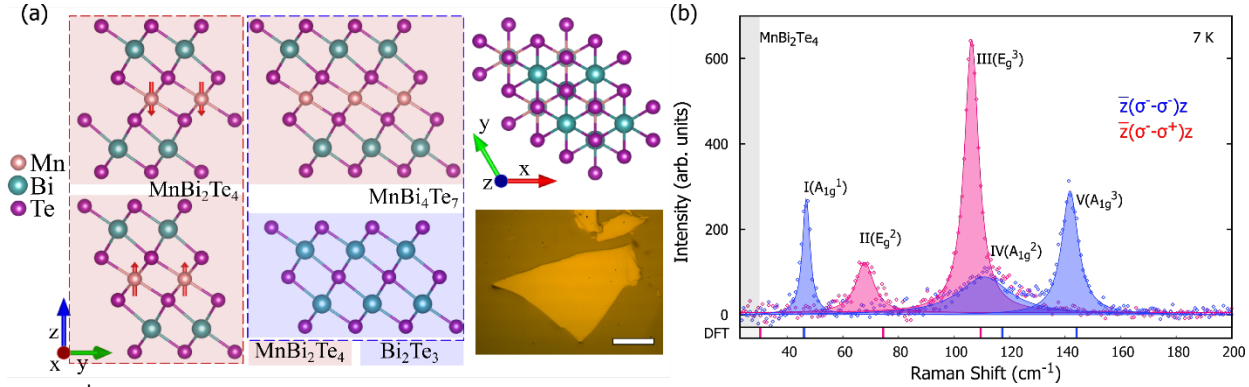

Figure 1 | (a) Crystal structure of $MnBi_2Te_4$ (left) and $MnBi_4Te_7$ (middle); and the top view of $MnBi_2Te_4$ (top right). An optical image of the exfoliated sample on silicon substrate. The scale bar is 20 μm. (b) Raman spectrum of $MnBi_2Te_4$ measured at 7K (top) and the Lorentzian fitting of each peak. Peak numbers are denoted as Roman numerals (I to V). Blue peaks represent A mode with $\sigma^- - \sigma^-$ and red peaks E mode with $\sigma^- - \sigma^+$ polarization measurement. The bottom bar shows the peak positions derived from DFT calculations in each polarization configuration. The gray shaded area indicates the cut-off filter frequency.

3. Results and Discussion

Figure 1 (b) shows Raman spectrum (top) of $MnTe_2Te_4$ with a total of five corresponding Lorentzian peaks of the phonon vibrational modes with the bar on the bottom representing the peak positions from DFT calculations. To observe each mode more clearly, we use a circular polarization configuration to distinguish E-mode (red) and A-mode (blue) of the peaks. Two peaks around 66 cm^{-1} and 112 cm^{-1} are governed by the oscillation of Mn-Te chains while the remaining peaks arise from the vibration of the top and bottom Bi-Te chains. The Raman peak position shifts are as we expected, consistent with an anharmonicity model including three-phonon scattering (Figure 2 (a)). According to this model, the widths of peaks are also speculated to be get narrower as temperature decreases as can be seen in peak V in Figure 2 (b). However, abnormal change in the linewidths of the former two peaks (IV and II) is observed as temperature decreases. Elaborating, peak IV is about 20% broader at the cryogenic temperature and peak II begins to broaden below 20 K which is near Néel Temperature (Figure 2 (b)-(c)). This broadening behavior cannot be explained with the anharmonicity model. Rather, it is attributable to the spin-ordering in Mn atoms altering the vibration of the Mn-Te chain while the remaining peaks (i.e., peaks I, III, V with peak V provided in figures for illustration purposes) come from the Bi-Te chain which is not directly bonded with Mn atoms.

In the case of $MnBi_4Te_7$, the insertion of another Bi_2Te_3 layer instigates Davydov splitting of the A_{1g} mode at 136 cm^{-1} at room temperature (Figure 2 (d)). The splitting becomes more distinguishable at cryogenic temperature, which fit two Lorentzian curves as can be seen in the inset of Figure 2 (d). Based on the linear chain model, we estimate the out-of-plane interlayer force constant to be 4.48×10^{19} N/m^3, which is three-times weaker than Bi_2Te_3. Building on insights into the underlying mechanism of the phonon modes and the layer interactions in the $MnBi_{2n}Te_{3n+1}$ series, additional properties of the $MnBi_{2n}Te_{3n+1}$ series will be investigated, such as pressure-induced changes of the transition temperature or IR-active vibrational modes, accompanied by neutron scattering.

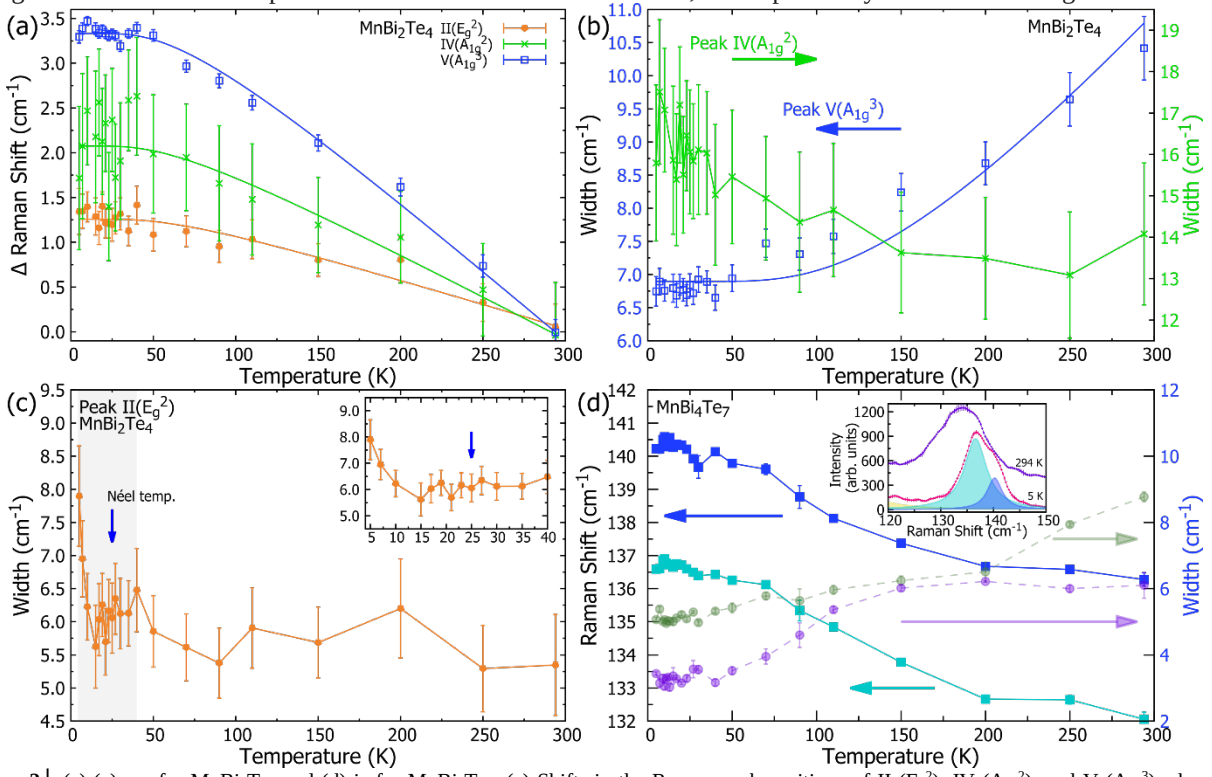

Figure 2 | (a)-(c) are for $MnBi_2Te_4$ and (d) is for $MnBi_4Te_7$. (a) Shifts in the Raman peak positions of II (E_g^2), IV (A_{1g}^2), and V (A_{1g}^3) when compared to the peak positions at room temperature. (b) Widths of peak V (A_{1g}^3) with left y-axis and peak IV (A_{1g}^2) with right y-axis in terms of temperature. Blue solid line in peak V (A_{1g}^3) is the fit with the anharmonicity model. (c) Temperature dependent width of peak II (E_g^2) indicating potential effect of spin-phonon coupling appearing below the Néel temperature (blue arrow). The shaded area, near the Néel temperature, is magnified in the inset. (d) Raman peak shift (left y-axis) and its width (right y-axis) of temperature dependent peak V (A_{1g}) splitting into two Lorentzian fittings of $MnBi_4Te_7$. The inset presents temperature dependent Raman spectrum focused on peak V (A_{1g}), 136 cm^{-1}. The two Lorentzian fittings at 5 K are depicted as light- and deep- blue curves.

4. References

[1] Tokura, Yoshinori, Kenji Yasuda, and Atsushi Tsukazaki. "Magnetic topological insulators." *Nature Reviews Physics* 1.2 (2019): 126-143.
[2] Otrokov, Mikhail M., et al. "Prediction and observation of an antiferromagnetic topological insulator." *Nature* 576.7787 (2019): 416-422.
[3] Hu, Chaowei, et al. "A van der Waals antiferromagnetic topological insulator with weak interlayer magnetic coupling." *Nature communications* 11.1 (2020): 1-8.
[4] Yan, J-Q., et al. "Crystal growth and magnetic structure of $MnBi_2Te_4$." *Physical Review Materials* 3.6 (2019): 064202.